

## RISK ESTIMATION TECHNIQUES IN CASE OF WPW SYNDROME

S. M. Szilágyi\*, Z. Benyó\*\*, L. Szilágyi\*\*

*\*Faculty of Technical and Human Science  
Sapientia – Hungarian Science University of Transylvania*

*\*\*Department of Control Engineering and Information Technology,  
Budapest University of Technology and Economics, Hungary*

Abstract: This paper presents a new non-invasive method to estimate the danger to which are exposed the patients suffering from Wolff-Parkinson-White (WPW) syndrome. Our aim is to provide reliable risk estimation, and to formulate its limitations. The first task is the localization of the accessory pathway (AcP), which we solved using the stepwise Arruda algorithm. After getting the AcP location it was possible to determine the pre-excitation time and rate. A total of 42 patients were studied, and an 88% localization performance was reached. This was considered quite good result compared with the highest published figures (90%) by Boersma in 2002. The highest pre-excitation time was  $92 \pm 5$ ms at a heart rate ( $HR=70 \pm 10$ ). Although we could not measure the repolarization time of the AcP, the obtained results can help to construct non-invasive patient risk estimation. *Copyright © 2005 IFAC*

Keywords: Heart wall motions, Medical applications, Models, Neural network, Real-time systems, Signal processing.

### 1. INTRODUCTION

#### *A. Medical background*

The Wolff-Parkinson-White syndrome is characterized by an accessory pathway (by-pass tract) between the atria and ventricles that conducts in parallel with the atrioventricular (AV) node - His bundle, but faster (Yee, *et al.*, 1995). An accessory AV connection can conduct in both directions. The presence of these by-pass tracts may predispose to atria-ventricular reentrant tachycardia. Moreover, in the setting of atrial fibrillation, the WPW syndrome can cause catastrophically rapid ventricular response with degeneration to ventricular fibrillation (VF).

Electrocardiographically the WPW syndrome can be characterized by a specific pattern in sinus rhythm, paroxysms of re-entry tachycardia (the incidence in the young adult population is about 10% and growing up with age to 30%) and more rarely by paroxysm of atrial fibrillation (20–30% of patients with the syndrome) or atrial flutter. In the case of WPW syndrome, the electrocardiogram (ECG)

tracing is a mixture of the electrical activities (Szilágyi, *et al.*, 2003a) caused by the accessory AV connection and normal AV conduction system. The fast impulse conduction produces an initial deflection in the QRS complex (delta wave – that event is shown in Fig. 3) (Szilágyi, *et al.*, 2003b). The length of this delta wave is determined by the difference between the accessory AV connection and normal AV conduction times. The modified ventricular activation causes secondary abnormalities in ventricular repolarization such as: ST segment displacement (elevation or depression), T wave shape distortion and abnormal U wave appearance. The accessory AV connection's conduction capacity variances can cause alternating WPW pattern, concertina effect, and episodic conduction. Changes may occur hour by hour or day by day.

An adequate analysis of this phenomenon is necessary, because 0.1-0.2% of the population suffer from WPW syndrome. When the accessory connection's refractory period is too short, the patient's life is in danger due to a possible VF.

Unfortunately the exact risk for developing VF during high ventricular rates is unknown. In consequence of the accessory connection's cells small mass, their electrical properties cannot be seen on an ordinary ECG measurement (with maximum 12-bit resolution).

### B. WPW syndrome analysis

Usually the WPW analysis is focused to develop and validate an AcP localization method. A number of investigations have correlated ECG patterns and algorithms for detecting the localization of the AcP (Arruda, *et al.*, 1998). Some study has been focused on the localization, realized through three-dimensional (3D)-heart reconstruction by the inverse solution of the ECG (Guanglin, *et al.*, 2001).

Several approaches have been explored to handle the problem of multiple solutions by using equivalent cardiac generators (such as equivalent dipole and multi-pole), heart surface isochrones, or epicardial potential (Shahidi, *et al.*, 1994). The high sensitivity of solutions to the different disturbances forced the investigators to explore regularization techniques. These methods allow a significant progress, but the different uncertainty elements of the processing limit the potentially beneficial ECG inverse solutions from becoming a routine clinical tool at present.

Body surface potential mapping (BSPM) was developed to allow an almost complete data acquisition from the body surface. The BSPM may have a great advantage over the standard 12-lead system in different situations due to deeper available information. Mirvis has shown some cases of BSPM recordings that demonstrate clearly the inadequacies of the standard ECG lead sets in a variety of pathologies.

In this paper we present a new method to identify the nature of WPW syndrome and to estimate its clinical relevance. A non-invasive classification is performed using 12 lead ECG recordings. Significant accuracy increment is obtained with BSPM. Hopefully, using BSPM and 16-bit resolution 12-lead ECG registrations, the dangerous and non-dangerous cases will be distinguishable, which improves the performance of WPW therapy, as it decides in a reliable manner whether an invasive interaction is needed or not.

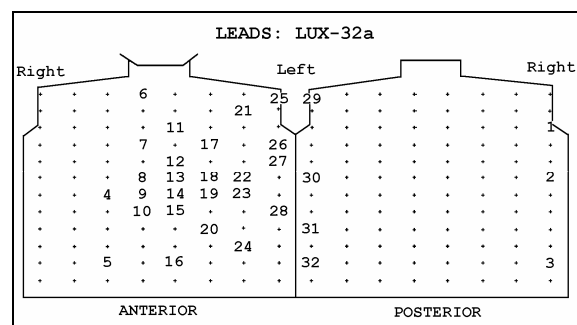


Fig. 1. Lux-32a electrode placement.

The morphology of the delta wave during sinus rhythm depends on the location of the ventricular insertion and the speed of activation propagation of the AcP. Our main purpose is to decipher the location and to determine the conduction speed of the ventricular insertion. From the localization and timing information we can estimate the pre-excitation rate. These parameters have a great contribution to develop a risk estimator analysis.

## 2. METHODS

### A. Study records

The first part of the study was performed on 42 patients referred for radio-frequency (RF) catheter ablation. Each ECG recording (more than 100 measurements altogether) was sampled using 12 leads, 12-16 bits resolution at 500-1000 Hz. The average age of the patients was 35 (15 to 70).

The second registration resource was a 32-electrode measurement (BSPM) database (sampled at 1000 Hz with 12-bit resolution) obtained from the Research Institute for Technical Physics and Materials Science (MTA-MFA) of Budapest. These measurements were collected using Lux-32a electrode placement (Lux, *et al.*, 1978). (see Fig. 1).

The selection of the limited 32-lead electrode subset from the original 192 regular lead arrangement was based on a statistical procedure focused to allow a low estimation error for the 160 unmeasured leads. Unfortunately the absence of additional information (for example RF catheter ablation) hindered us to verify the Arruda localization method with these measurements.

### B. Localization

Our first task in WPW syndrome analysis was to determine the location and nature of the accessory connection. As the standard 12-lead ECG recordings held most of the desired information, we could locate the AcP from our measurements.

We preferred to solve this localization with Arruda's stepwise method instead of the Fitzpatrick algorithm (the Arruda algorithm is presented in Fig. 5). The clinically tested and well-known Arruda method had used only five leads (I, II, III, aVF, V1) from the 12-lead ECG recordings. However this localization method could reach 90% recognition rate, some modification in this place identification algorithm could be benefic.

Starting from the stepwise method of Arruda, we had to determine its performance and eventually to propose some modifications. The possible AcP locations were divided into three major regions, which were further divided thereafter, as follows:

- Septal accessory pathways: anteroseptal tricuspid annulus and right anterior paraseptal (AS/RAPS), mid-septal tricuspid annulus (MSTA), posteroseptal tricuspid annulus (PSTA), posteroseptal mitral annulus (PSMA), subepicardial posteroseptal (SEC);
- Right free-wall accessory pathways: right anterior (RA), right anterolateral (RAL), right lateral (RL), right posterolateral (RPL), right posterior (RP);
- Left free-wall accessory pathways: left anterolateral (LAL), left lateral (LL), left posterolateral (LPL), left posterior (LF).

These major and minor locations were illustrated in Fig. 2., indicating the place of the His bundle (HIS).

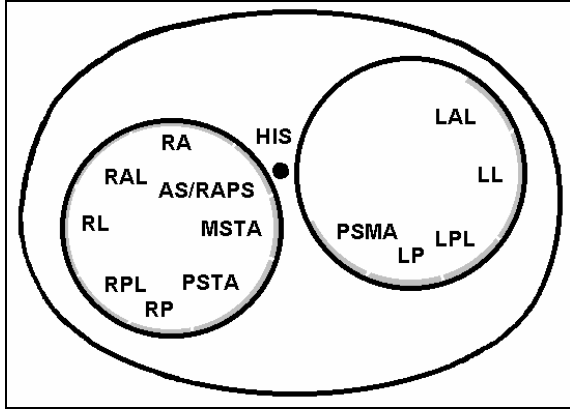


Fig. 2. Schematic representation of the heart as viewed in the left anterior oblique projection.

The starting points of our WPW analysis were the study of delta wave and QRS complex mixture. We had to analyze the amplitude relations of the R, S and delta ( $\Delta$ ) waves in order to determine the AcP location.

The onset of the delta wave in each lead was measured from the onset of the earliest delta wave in any of the 12 leads. After 20 ms the displacement of the delta wave in each lead was classified as positive (+), negative (-) or isoelectric (0).

To provide a smoother decision we adapted the comparisons and yes/no decisions of the Arruda method to probabilistic transform functions. A genetic algorithm had to set up these heart rate (HR) dependent  $f_{lead}^{\Delta}(HR)$  and  $f_{lead}^{R-S}(HR)$  functions.

### C. Pre-excitation time estimation

After getting to know the AcP location it became possible to determine the pre-excitation time and rate. These estimations are based on the shape of the delta wave in different leads. In order to determine the conduction speed of the AcP, we had to introduce some terms related to conduction timings:

- $\tau_{SA-AP}$ : Time elapsed from propagating the sinus impulse to the accessory AV connection;

- $\tau_{SA-AV}$ : Time elapsed from propagating the sinus impulse to the AV node;
- $\tau_{AV}$ : Conduction time of AV node-His bundle path;
- $\tau_{AP}$ : Conduction time of accessory AV connection;
- $\tau_{SA-V} = \tau_{SA-AV} + \tau_{AV}$ : Time elapsed from propagating the sinus impulse to ventricular area (PQ interval in case of normal ECG);
- $\tau_{Adv} = \tau_{SA-V} - (\tau_{SA-AP} + \tau_{AP})$ : Time differences from excitation of ventricular area from accessory pathway and AV node-His bundle path;
- $\tau_*$ : The global notation of the above mentioned times.

All conducting periods depended on a lot of external and internal parameters such as: HR, environmental influence, medicament effects, and general condition. The effect of these circumstances, which were influential, could not be determined or deducted due to the high number of unknown coefficients, so the average effect of these things could be estimated only empirically (the usage of further clinical measurements should increase the estimation performance). In our paper, we had to separate the effect of HR and other influential factors, due to a much deeper knowledge about HR's behavior.

The most important and measurable parameter we used at the determination of the  $\tau_*$  conduction times was HR. We considered  $f_{\tau_*}(HR)$  the description function of the conducting times ( $\tau_*$ -s) for different heart regions (compartments). These values were determined by the formula

$$f_{\tau_*}(HR) = \frac{1}{n} \sum_{i=0}^{n-1} \sum_{j=0}^{k-1} c_*(i, j, HR) \cdot p_*(i, j, HR),$$

where  $p_*(i, j, HR)$  denoted the internal and external influential parameters (i denotes the compartment, j the different factors) with coefficients  $c_*(i, j, HR)$ .

By applying the estimated coefficients, we determined the AcP conduction time  $\tau_{AP}(HR) = \tau_{AP}(norm) \cdot f_{\tau_{AP}}(HR)$  for different HR-s, where  $\tau_*(norm)$  represents  $\tau_*$  at a pre-set HR (in our case 70 beat/min).

The inflexion point detection of the  $\Delta - R$  wave was an unavoidable step in  $\tau_{Adv}$  determination. The investigation should include all leads (cannot be restricted only to a specific lead, for example V3), due to the following reasons:

- The location of the AcP influences in differently way the  $\Delta - R$  wave detection

possibilities at the measuring electrodes (the detection is lead dependent);

- The lead, where the  $\Delta - R$  wave appears for the first time, depends on both the patient and the internal state.

A regressive identification method determined the “best fitting” sample. The wave’s starting time was considered the moment when it first appeared in any of the leads.

Starting from the above mentioned facts, we obtained the formula

$$\tau_{AP}(HR) = \frac{\tau_{SA-AV} \cdot f_{\tau_{SA-AV}}(HR) + \tau_{AV} \cdot f_{\tau_{AV}}(HR)}{f_{\tau_{AV}}(HR)} - \frac{\tau_{Adv} \cdot f_{\tau_{Adv}}(HR) - \tau_{SA-AP} \cdot f_{\tau_{SA-AP}}(HR)}{f_{\tau_{AV}}(HR)}$$

#### D. The impact of body surface potential maps

In order to improve the accuracy of the procedure, we had to use the BSPM samples due to the significantly more information, than the 6 or 12-lead records. However most BSPM lead sets contain significant amounts of redundancy, this information we could use to minimize measurement errors. Low measurement error is crucial in inverse ECG reconstruction.

From the BSPM measurements we evaluated the followings:

- The depolarization wave spatial propagation from the arrangement of the electrodes;
- Earlier  $\Delta$  wave appearance in BSPM, than in case of standard 12-lead ECG;
- Measurement error analysis from redundant information.

Having considered  $L_{AP}(x, y, z)$  the location in space of the AcP (the last fraction of AcP before depolarizing ventricles),  $L_{E(i)}(x, y, z)$  the location in space of the  $i^{\text{th}}$  electrode, and  $L_{E(\text{first})}(x, y, z)$  the location of the first  $\Delta$  wave onset, we could deduce the average angle between the depolarization wave and measuring electrode. The onset of the  $\Delta$  wave was considered more accurately detectable in BSPM, then in case of standard 12-lead ECG, due to its higher number of electrodes. To obtain a description formula we had to use a 3D heart depolarization model, whose details are not included in the topic of this paper.

#### E. Depolarization analysis

We wanted to estimate the depolarization rate from AcP and AV. Some of the possible solutions are listed below:

- When the inflexion point in  $\Delta - R$  wave was determined, it was likely to calculate the pre-excitation rate from  $\Delta$ ,  $R$  and  $S$  amplitudes;

- The ventricular tissue mass (depolarized from AcP) was estimated using depolarization wave analysis in time for BSPM records.

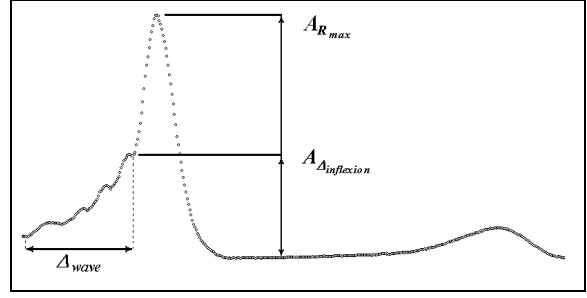


Fig. 3. Schematic representation of the pre-excitation rate estimation.

The pre-excitation rate could be determined by formula  $\eta_{Ampl} = A_{\Delta_{inflexion}} / A_{R_{max}}$ , where  $A$  represents amplitudes (see Fig. 3).

Let  $t_{AP}$  be the time of  $\Delta$  wave onset (first appearance of  $\Delta$  wave at any electrode) and  $t_{inflexion}$  the time when we detected the inflexion point in  $\Delta - R$  wave. We considered the depolarization intensity to be linearly proportional with the maximal value of  $\Delta - R$  wave at any electrode.

Due to a rapid depolarization speed of a ventricular myocardial cell (the action potential increases at least 100 times faster in phase 0 than decreases in phases 1-4), we took in consideration only phase 0 from myocardial action potential function.

From the above considerations ( $t_{AP}$ ,  $t_{inflexion}$ , action potential function) we could determine the tissue mass depolarized from AcP by formula

$$m = c \cdot \sum_{i=t_{AP}}^{t_{inflexion}} (\Delta - R)_{\max(i)},$$

where  $c$  denotes a proportional coefficient (determinable from a normal and pre-excitation beat analysis), and  $(\Delta - R)_{\max(i)}$  represents the measured maximal value in time  $i$  at any electrode (the depolarization wave changes its direction in time). The pre-excitation rate with mass analysis was determined by the formula

$$\eta_{Mass} = m / m_{Ventricular}.$$

As we mentioned earlier, in this paper we did not use 3D heart model and repolarization analysis (T wave), so the last two ways of estimation were omitted.

### 3. RESULTS

We considered important to represent the relationship between the predicted and actual (based upon ablation site) distribution of AcP location (see in Table I). Ablation sites are represented in vertical and the predicted locations in horizontal direction.

**Table 1 Location and detection accuracy of the accessory pathway**

Ablation Site	Number	RA/RAL	RL	RP/RPL	AS/RASP	MSTA	PSTA	PSMA	LP/LPL	LL/LAL	SEC	%
RA/RAL	6	6										100
RL	4	1	3									75
RP/RPL	3			3								100
AS/RASP	1				1							100
MSTA	2					2						100
PSTA	8					1	6		1			75
PSMA	0											NA
LP/LPL	1								1			100
LL/LAL	12								2	10		83
SEC	5										5	100
All	42											88

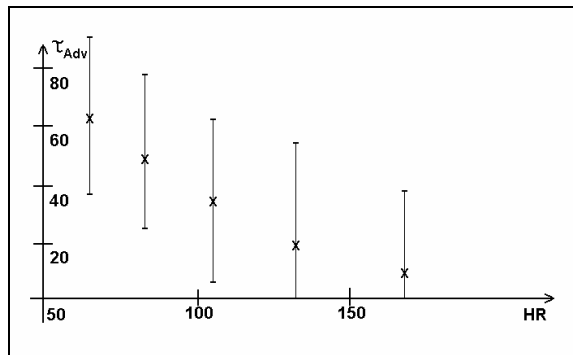


Fig. 4. Time differences (represented in ms) of ventricular area depolarization from AcP and AV node-His bundle path (average and extreme values) in function of HR.

The average and extreme values of  $\tau_{Adv}$  (represented in ms) for different HR were illustrated in Fig. 4. The origin was placed at 50 beat/min and 0 ms. From the approximately 1000 BSPM registrations 14 held WPW. These samples were analyzed and the pre-excitations times and rates (amplitude and mass estimation) were determined (see in Table II).

**Table 2 Pre-excitation times and rates**

Record no.	$\tau_{Adv}$	$\eta_{Ampl}$	$\eta_{Mass}$
368	32.4	0.1017	0.063
369	83.8	0.8176	0.799
370	84.8	0.4343	0.378
371	21.6	0.1714	0.145
372	18.5	0.0723	0.047
373	22.8	0.2128	0.144
374	20.7	0.5904	0.390
375	10.1	0.2593	0.226
376	66.3	0.1900	0.118
377	8.2	0.0518	0.026
378	73.9	0.3095	0.237
379	70.8	0.8162	0.804
380	24.8	0.8860	0.901
381	64.2	0.8658	0.843

#### 4. DISCUSSION

The Lux-32a electrode placement contains too few electrodes on the back side. So the localization performance on the posterior region is slightly lower, which is reflected in Table 1.

After we had analyzed the Arruda AcP localization algorithm, we observed that most times the estimation errors were correlated with aVF+ test. In the graphical representation of the localization algorithm (see in Fig. 5) the sensitive spots (all of them represent aVF+) are encircled. In our study 80% of the prediction errors were caused by a weak aVF+ decision (see in Table I).

The localization made by simple comparison shows lower recognition percentage in case of RL, PSTA, and LL/LAL locations. In case of PSTA the  $R \geq S$  relation in  $V_I$  and aVF- could happen, so these restrictions do not imply in all cases LP/LPL.

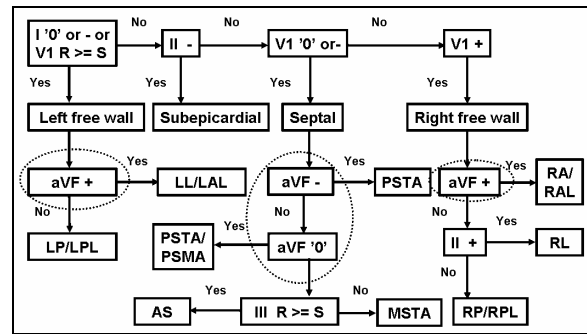


Fig. 5. Stepwise Arruda method for determination of AcP location

These observations must be used with care due to the followings:

- Our database was too small to guarantee a solid statistical confirmation;
- The selected patients were not 100% representative (due to the small number);
- We used only few recordings from one patient, so the WPW syndrome could manifest in other way (it could change its behavior hourly).

Several attempts had been made to correlate ECG findings with anatomic locations of accessory AV pathways in patients with WPW syndrome. The processing method differs from prior algorithms in its capability to determine the locations, time differences, and pre-excitation rates at the same moment. The 88% recognition rate we considered quite good, compared with the highest published value of 90% (Boersma, *et al.*, 2002). Reconstructing the inner structure of the heart we made errors in case of RL, PSTA, LL and LAL. Slight modifications in reconstruction must still be made to increase the performance of the method.

The location of accessory pathway determines  $\tau_{SA-AP}$  and can influence the shape of T wave, too.

Due to a slower depolarization speed (determinable from  $\Delta$  wave's shape) and epicardial junction place (determinable from modified T wave shape) from accessory pathway, the conduction speed is deductible using the size and location of depolarized ventricular area from accessory AV connection.

Analyzing the time differences (Szilágyi, *et al.*, 2003b) (see in Fig. 4) from excitation of ventricular area from AcP and AV node-His bundle path, we can consider that  $\tau_{Adv}$  is inverse proportional with heart rate. The highest  $\tau_{Adv}$  value was  $92 \pm 5$ ms (HR =  $70 \pm 10$ ), but at high heart rate the  $\tau_{Adv}$  can reach zero (HR > 130).

Further considered methods for depolarization analysis, which have not yet been tested due to technical difficulties, are listed below:

- From a 3D heart model and the measured ECG it was possible to construct a depolarization model. The pre-excitation rate was considered the rate of ventricular tissue depolarized from AcP and respectively AV;
- With the help of repolarization (T wave distortion) it was possible to determine the process of depolarization.

From the data presented in Table II, it is possible to deduce a high dispersion of  $\eta_{Ampl}$  and  $\eta_{Mass}$  in function of  $\tau_{Adv}$ , which is caused by the influence of unknown parameters that determine the shape of the ECG signal. As the pre-excitation time increases, the dispersion had a slight decrement.

We observed that high  $\tau_{Adv}$  with high  $\eta_{Ampl}$  or  $\eta_{Mass}$  represent a risk factor. Unfortunately the obtained information is not enough to construct a completely non-invasive and efficient risk estimation method, because of the unknown repolarization behaviour (repolarization time in function of HR) of the accessory connection's cells. The repolarization properties cannot be determined non-invasively without using 16-bit resolution ECG measurement system.

Making a comparison between locations and time advances needs much more measurements, so this is one of our future tasks. A heart-model-based localization (Szilágyi, *et al.*, 2003a) can increase the recognition performance. With high accurate measurements (at least 16 bits resolution) there exists a theoretical chance to determine the repolarization time of accessory connection's cells.

High  $\eta_{Ampl}$  and  $\eta_{Mass}$  represents a risk for the patient, but the danger can be estimated only with low accuracy. A lot of empirical parameters (patient age, physical condition) also influence the risk factor. These considerations create the foundation of a reliable patient risk estimator method based on non-invasive procedures.

## ACKNOWLEDGEMENT

The authors would like to thank Mr. György Kozmann, expert in biomedical engineering with the Research Institute for Technical Physics and Materials Science, Budapest, Hungary, Mr. Attila Frigy, physician at Medical Clinic No. 4 of Tirgu Mures, Romania, for their help provided for this study. The research has been supported by the Hungarian National Research Fund (OTKA), Grants T029830, T042990, Sapientia KPI, and Domus Hungarica.

## REFERENCES

- Arruda M., McClelland J., et al (1998), Development and Validation of an ECG Algorithm for Identifying Accessory Pathway Ablation Site in Wolff-Parkinson-White Syndrome, *J Cardiovascular Electrophysiology*, **9**, pp. 2-12.
- Benyó B., Asztalos B., (2000), Detection of Pathologic Alterations of the Heartwall Based on Ultrasound and Echocardiographic Pictures, *ORKI Medical and Hospital Engineering*, vol. **XXXVIII**, No. 2., pp. 36-40.
- Boersma L., Moran E., Mont L., Brugada J. (2002), Accessory pathway localization by QRS polarity in children with Wolff-Parkinson-White syndrome., *Journal Cardiovasc Electrophysiol.* **13**(12), pp. 1222-1226.
- Guanglin L., Bin H. (2001), Localization of the Site of Origin of Cardiac Activation by Means of a Heart-Model-Based Electrocardiogr. Imaging Approach, *IEEE Trans. BME*, **48**, pp. 660-669.
- Lux R. L., Smith C. R., Wyatt R. F., Abildskov J. A. (1978), Limited lead selection for estimation of body surface potential maps in electrocardiography, *IEEE Trans. BME*, **25**, pp. 270-276.
- Shahidi A. V., Savard P., and Nadeau R. (1994), Forward and inverse problems of electrocardiography: Modeling and recovery of epicardial potentials in humans, *IEEE Trans. Biomed. Eng.*, vol. **41**, pp. 249-256.
- Szilágyi S.M. (2000), The Limits of Heart-Model-Based Computerized ECG Diagnosis, *World Congress on Medical Physics and Biomedical Engineering*, Chicago, pp. 1913-1916.
- Szilágyi S. M., Benyó Z., Dávid L. (2003a), Heart Model Based ECG Signal Processing, *5<sup>th</sup> IFAC Symposium on Modelling and Control in Biomedical Systems*, Melbourne, pp. 213-217.
- Szilágyi S. M., Benyó Z., Dávid L. (2003b), WPW Syndrome Identification And Classification Using ECG Analysis, *World Congress on Medical Physics and Biomedical Engineering*, Sydney, Australia, paper #4423.
- Yee R., Klein G. J., Guiraudon G. M. (1995), The Wolff-Parkinson-White syndrome, In: *Cardiac electrophysiology. From cell to bedside*. Philadelphia: WB Saunders Co, pp.1199-1214.